

THE INTERACTION BETWEEN ELECTROMAGNETIC RESONANCES AND ITS ROLE IN SPECTROSCOPIC STUDIES OF MOLECULES ADSORBED ON COLLOIDAL PARTICLES OR METAL SPHERES

P.K. ARAVIND

Department of Chemistry, University of California, Santa Barbara, California 93106, USA

Abraham NITZAN

Department of Chemistry, Tel Aviv University, Tel Aviv, Israel

Horia METIU *

Department of Chemistry, University of California, Santa Barbara, California 93106, USA

Received 17 February 1981

We study the modification of optical properties of two metal spheres brought about by their electromagnetic interactions. We compute the excitation spectrum of the two sphere system and study the shape and the magnitude of the local fields. The relevance of this calculation to surface enhanced spectroscopy and to the study of the Brownian motion in colloidal solutions is discussed.

1. Introduction

Recently there has been experimental [1–6] and theoretical [7–12] interest in the use of electromagnetic resonances to influence the spectroscopy of molecules placed on or near “rough” surfaces. The excitation of a localized resonance, by photon absorption, packs the photon energy in a small spatial region, thus increasing the local electromagnetic field. A molecule positioned in such a region is polarized by an electric field E which is enhanced with respect to the incident laser field. The enhancement of the quantity $E \cdot E$, which is of importance in most spectroscopic measurements, can be as much as ten thousand. Generally, this results in a dramatic increase of the desired spectroscopic signal. Recent works have suggested that such enhanced local fields may even be useful in influencing dynamic processes, such as photon induced desorption [13] or photochemical decomposition [14].

Besides enhancing the local field an electromagnetic resonance may also affect spectroscopy by coupling to the polarized molecules. This causes energy exchange between the excited molecule and the resonance, which modifies the fluorescence life-time and intensity [15], the molecular absorption line-shape [15] and the resonant Raman intensity [16].

* A.P. Sloan Fellow and Camille and Henry Dreyfus Teacher Scholar.

Among the systems that permit the use of electromagnetic resonances for the modification of the spectroscopy of adsorbed molecules, colloidal solutions have some distinct advantages. They are stable and easy to prepare. The size distribution is fairly uniform and the particle shapes tend to be close to spherical. Varying the method of preparation one can change the particle sizes and their distribution in a reproducible manner. Flowing the sample minimizes both the surface damage by the laser and the effect of the photochemical decomposition of the molecules. They are appealing to the theorist since they are easier to model than all other systems except perhaps the holographic gratings. Most of the electrodynamic calculations can be carried out exactly.

The interest in such systems is further stimulated by the fact that the electromagnetic (i.e. optical) properties of very small metal particles is a traditional subject with a number of unresolved questions. It is not yet clear to what extent their dielectric constant is size dependent [17]; the role of spatial dispersion is not understood; there are some unexplained phenomena, such as the observed [18] enhancement of the photo-electric yield and its pronounced size dependence. The use of measurements of spectroscopic properties of molecules located near such particles, could provide additional ways of testing the quality of various assumptions concerning the optical response of the particles.

The experimental studies [6] of enhanced Raman scattering for molecules absorbed on Ag and Au colloids have produced results that are qualitatively congruent with the idea that the enhanced Raman signal is caused by the excitation of the electromagnetic resonance of the sphere. For example, the dependence of the Raman signal intensity on the frequency of the incident laser follows the absorption curve of the colloid particle. No Raman signal is observed in a frequency range in which the turbidity is high but it is caused by scattering off the forward direction, rather than absorption by the resonance.

However a detailed comparison between theory [8b] and experiment [6b] for Ag colloids shows enough discrepancies to cause some concern. If the computed absorption curve for isolated colloidal spheres is adjusted to have the same maximum as the observed one (by adjusting the particle radius) one finds that the shapes of the computed and measured absorption curves are different. The computed absorption curve is a narrow Lorentzian while the observed one is much broader and has an even broader shoulder extending in the low frequency region. Furthermore, the calculated excitation spectrum in the range of wavelength from 350.7 to 647.1 nm has a peak, while the observed one grows rapidly in the low wavelength region and levels off towards the higher values.

The origin of these discrepancies is not clear. They may be caused by experimental problems, such as colloid aggregation, particle polydispersity, or non-sphericity. Furthermore, it is not certain that the dielectric constant of the colloid particles is the same as that of the bulk metal; size effects as well as structural and/or chemical differences between the colloid and the bulk metal, may cause some differences.

In this paper we want to point out that some interesting effects are caused by the interaction between resonances located on two spheres. It is well known that the local fields produced by resonance excitation in one sphere extend quite far ($\sim 100 \text{ \AA}$) into the solution. The interaction between two such spheres takes place through the electromagnetic field whose energy at a point r is proportional to $E(r) \cdot E(r)$. Since the total field at r is $E(r) = E_1(r) + E_2(r)$, where $E_i(r)$ is the field caused at r by the resonant excitation of the sphere i , the field Hamiltonian will contain a term of the form $E_1(r) \cdot E_2(r)$, which represents the interaction Hamiltonian between the two resonances. Since both $E_1(r)$ and $E_2(r)$ are sizable at distances of roughly 100 \AA from the edge of the corresponding spheres, the interaction is very long ranged. Therefore resonances on spheres separated by as much as 150 \AA interact with each other.

Since one can think of the two resonances as two degenerate harmonic oscillators (in the Rayleigh limit or when the two spheres are of equal size) the long range coupling may cause substantial shifts of the resonant frequencies. The degenerate "modes" are replaced by two new ones (which are the experimentally observable ones) having two different frequencies; one is much lower than the frequencies of the isolated spheres and the other is close to it. Therefore, the excitation spectrum should have a double hump and the peak positions vary with the distance between the spheres. This splitting of the degenerate resonances should appear even when the spheres are separated at substantial distances.

This phenomenon has interesting implications for the spectroscopy of molecules located in colloidal solutions, if the colloid concentration is sufficiently large to allow the existence of a large number of pairs whose separation is smaller than the distance required for a sizable interaction between resonances. In such a case the excitation spectrum (of the resonances – hence of the Raman line) is modified and will acquire a low frequency component, which is absent in the infinite dilution limit (when the spheres do not interact).

Furthermore, we expect (and find) that the fields in the region between the spheres is larger than the sum of the fields caused by two non-interacting spheres located at the same interparticle separation. In other words, there is a cooperative effect caused by the mutual polarization of the interacting spheres. Thus the interaction between the spheres will have two effects: (a) It will permit a sizable Raman signal at frequencies lower than the ones required for the excitation of the isolated spheres; (b) At the frequency at which the isolated spheres can be excited one obtains larger local fields (hence spectroscopic signals) acting on the molecules located between spheres.

The interaction between resonances may also be useful in the study of the Brownian motion of an ensemble of colloid particles. As the particles wander around, they will absorb at frequencies below those of the resonances of the isolated spheres whenever they come within a distance smaller than the interaction distance. In principle, a study of the absorption and its fluctuations (in the smallest possible illuminated volume) at many such low frequencies should allow one to ob-

tain some information about the average pair distribution function as well as the dynamics of the interparticle distance fluctuations, caused by the Brownian motion.

Finally, we emphasize that the problem of the interaction between localized electromagnetic resonances is of basic importance for all spectroscopic measurements on surface molecules, which use the enhancement caused by localized surface resonances. The theoretical models are usually developed for isolated resonances, sustained by non-interacting bodies of regular shape. The experiments are done in the opposite limit, using materials in which the resonant centers are fairly crowded and some (or a lot) of interaction between the resonances located on these centers is expected. Some very crude argument can be made to suggest that the effect of these interactions may be dramatic. An excited resonance turns on such a high local field because the energy of the absorbed photon is packed into a small spatial region. If many such resonance sustaining centers are brought together, the interaction between resonances spreads the photon energy among all these centers; therefore energy per unit volume (hence the local field) tends to be diminished. Consider, for example, a small isolated cube. Without doing any calculations it is clear that the isolated cube must have a resonance with a fairly large local field, which a photon can excite. However, if we take a large number of such cubes and pack them closely, we can construct a flat metal surface which (if thick enough) has only two resonances: the bulk and the surface plasmon. None of these can be directly excited by photons and therefore are not useful (unless an ATR configuration [5] is employed) in enhancing the signals in surface spectroscopy. This "close packing" example is an extreme and rather idealized case, which illustrates the fact that the interaction between resonances and the delocalization thus induced may have dramatic spectroscopic effects. We view the present calculation as a starting step towards a study of this delocalization problem.

2. The model

We consider two spheres of equal radius, as shown in fig. 1. For simplicity we confine ourselves to the Rayleigh limit, in which the size of the object is small compared to the radiation wavelength. This allows us to neglect retardation and therefore solve the Laplace equation, rather than Maxwell's equations. The solution can be obtained numerically with relative ease, since the equation is separable if bispherical coordinates [19] are used.

We chose the z -axis along the line passing through the centers of the spheres. The xy plane contains the mid-point between the spheres. The bispherical coordinate system (μ, η, ϕ) is chosen [19] so that the xy plane is located at $\mu = 0$ and the two spheres at $\mu = \pm\mu_0$. The parameter μ_0 and the length scale c_0 (denoted a in Morse and Feshbach [19]) are determined by R_0 and D (see fig. 1).

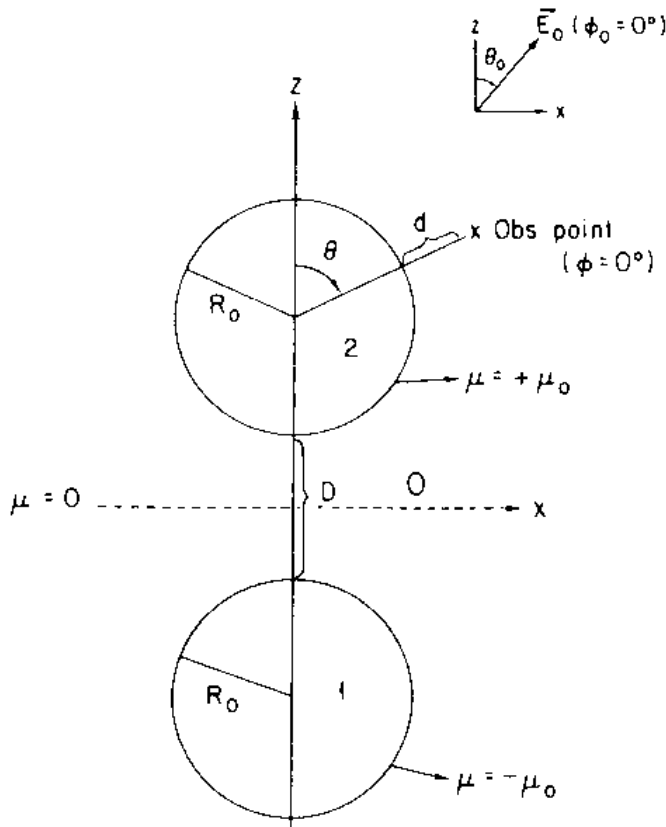


Fig. 1. Geometry of the 2-sphere system. Shown here are the relative dispositions of the two spheres, the orientation of the external field E_0 and the observation point at which the field enhancement is calculated.

We seek a solution of the Laplace equation of the form

$$\Phi_0 = \Phi^{\text{ext}} + F \sum_{n \geq |m|} \sum_{m=-\infty}^{\infty} \{A_n^m \exp[(n + \frac{1}{2}) \mu] + B_n^m \exp[-(n + \frac{1}{2}) \mu]\} Y_n^m(\cos \eta, \phi),$$

$$-\mu_0 < \mu < \mu_0, \tag{1a}$$

$$\Phi_2 = F \sum_{n \geq |m|} \sum_{m=-\infty}^{\infty} C_n^m \exp[-(n + \frac{1}{2}) \mu] Y_n^m(\cos \eta, \phi), \quad \mu > \mu_0, \tag{1b}$$

$$\Phi_1 = F \sum_{n \geq |m|} \sum_{m=-\infty}^{\infty} D_n^m \exp[(n + \frac{1}{2}) \mu] Y_n^m(\cos \eta, \phi), \quad \mu < -\mu_0. \tag{1c}$$

The spherical harmonics $Y_n^m(\cos \eta, \phi)$ are defined as in Jackson's book [20]. The factor F is equal to $(\cosh \mu - \cos \eta)^{1/2}$ and Φ_0, Φ_1 and Φ_2 are the potentials in the vacuum and the spheres 1 and 2, respectively. The external potential is

$$\Phi^{\text{ext}} = -E_0(z \cos \theta_0 + x \sin \theta_0 \cos \phi_0 + y \sin \theta_0 \sin \phi_0) \exp(-i\omega t). \tag{2}$$

This corresponds to an electric vector of magnitude $E_0 \exp(-i\omega t)$ directed along the polar angle θ_0 and the azimuthal angle ϕ_0 . These parameters are specified when

the frequency, the intensity and the direction of propagation of the laser beam are given.

The coefficients A_n^m , B_n^m , C_n^m and D_n^m are determined by requesting that Φ_0 , Φ_1 and Φ_2 satisfy the boundary conditions:

$$\Phi_0|_{\mu=\mu_0} = \Phi_2|_{\mu=\mu_0}, \quad (3a)$$

$$\Phi_0|_{\mu=-\mu_0} = \Phi_1|_{\mu=-\mu_0}, \quad (3b)$$

$$\epsilon_0 \left. \frac{\partial \Phi_0}{\partial \mu} \right|_{\mu=\mu_0} = \epsilon(\omega) \left. \frac{\partial \Phi_2}{\partial \mu} \right|_{\mu=\mu_0}, \quad (4a)$$

$$\epsilon_0 \left. \frac{\partial \Phi_0}{\partial \mu} \right|_{\mu=-\mu_0} = \epsilon(\omega) \left. \frac{\partial \Phi_1}{\partial \mu} \right|_{\mu=-\mu_0}. \quad (4b)$$

Here the dielectric constant of the metal is denoted $\epsilon(\omega)$ and that of the medium (taken here to be vacuum) is ϵ_0 .

Using the eqs. (1) through (4) we obtain – after some tedious algebra – an infinite linear system of equations for the coefficients A_n^m , B_n^m , C_n^m and D_n^m . This is given in the appendix. This system is truncated (by taking a finite maximum value n_{\max} for n) and solved on the computer. Special care must be taken to make sure that convergence is achieved (i.e. that n_{\max} is not too small).

Once these coefficients are obtained we compute the components of the electric field from

$$E_i = (1/h_i) \partial \Phi_0 / \partial i, \quad i = \mu, \eta, \phi; \quad (5)$$

here the quantities h_i (i.e., h_μ , h_η and h_ϕ) are the scale factors for the bispherical coordinates. It would be extremely cumbersome – and perhaps not worth the effort – to plot all these field components. For isotropic molecules the quantity of interest in spectroscopy is the scalar

$$I \equiv E_\mu E_\mu^* + E_\eta E_\eta^* + E_\phi E_\phi^*, \quad (6)$$

which is proportional to the “local intensity” incident on a molecule located near the spheres. The ratio

$$\tilde{I} = I / (E_0 E_0^*) \quad (7)$$

is a local enhancement factor which will appear, for example, in a computation of the enhancement of the Raman signal, for isotropic molecules (if the “image field” effects, which change the polarizability, not the local intensity [15,16], are neglected).

Before presenting numerical results it is instructive to specify how various physical quantities enter into the problem. We are interested in the fields in vacuum, therefore we want to know A_n^m and B_n^m .

There are symmetry elements in the problem that can be exploited. Since the two sphere system has a rotation axis its response to external fields can be analysed by using eigenfunctions of the projection L_z of the angular momentum operator on that axis. The external field can also be expressed in terms of a linear combination of angular momentum eigenfunctions by using the equations

$$|z\rangle = \sqrt{2cF} \sum_{n=0}^{\infty} [4\pi(2n+1)]^{1/2} \exp[-(n+\frac{1}{2})|\mu|] Y_n^0, \tag{8}$$

and

$$\begin{pmatrix} x \\ y \end{pmatrix} = \begin{pmatrix} -1 \\ 1 \end{pmatrix} \sqrt{2cF} \sum_{n=1}^{\infty} \left(\frac{4\pi n(n+1)}{(2n+1)} \right)^{1/2} \exp[-(n+\frac{1}{2})|\mu|] \begin{pmatrix} Y_n^1 - Y_n^{-1} \\ Y_n^1 + Y_n^{-1} \end{pmatrix}. \tag{9}$$

If the external field is directed along the z -axis then Φ^{ext} is proportional to z , and it is an eigenvalue of L_z , with $m = 0$. Due to symmetry the total field must also be an eigenvalue of L_z with $m = 0$, therefore all B_n^m and A_n^m with $m \neq 0$ must vanish. If the field is perpendicular to the z -direction the potential Φ^{ext} contains a term proportional to x and one proportional to y . Since these are linear combinations of eigenvectors of L_z with $m = +1$ and $m = -1$, the total potential must have the same properties; hence all the coefficients A_n^m and B_n^m are zero, except for those with $m = \pm 1$. For the intermediate angles of incidence only A_n^m, B_n^m with $m = 0, \pm 1$ survive.

In order to obtain the coefficients A_n^m, B_n^m we must solve the linear systems shown in the appendix. The matrix that must be inverted is independent on the direction of incidence of the field or on the point where the field is computed. It depends on frequency through the dielectric constant of the metal, which always enters through the combination $\chi(\omega) = [\epsilon_0 - \epsilon(\omega)] [\epsilon_0 + \epsilon(\omega)]^{-1}$. It also depends on the geometry through the parameter $\lambda = R_0/(2R_0 + D)$ (see fig. 1).

Resonances appear at frequencies at which any of the elements of the inverse matrix discussed above become very large. Since the matrix depends on χ and λ – but not on the properties of the exciting field (e.g., its direction or magnitude) or the position of the point where the total field is measured – the resonance frequency depends on the geometrical parameter λ and the nature of the metal (through $\chi(\omega)$) only.

3. Numerical results

The only serious numerical problem is related to the convergence of the calculation as n_{max} is increased. We find that as λ gets closer to 0.5 (i.e. the spheres get closer) the convergence worsens. In some cases we needed an n_{max} as large as 60. We emphasize that one cannot conclude that the basis set is large enough from the

fact that the sequences $\{A_n^m\}_{n=1}^{n_{\max}}$ and $\{B_n^m\}_{n=1}^{n_{\max}}$ are rapidly convergent. The value of the coefficients depend strongly on n_{\max} if the latter is not large enough.

To ensure that the basis set is sufficiently large we have taken the following precautions. (1) We increase the basis set until the sequences $\{A_1^m, \dots, A_{n_{\max}}^m\}$ and $\{B_1^m, \dots, B_{n_{\max}}^m\}$ are unchanged as n_{\max} is increased. (2) We test to make sure that the computed quantity (e.g. \tilde{I}) does not change with n_{\max} . (3) We compute, with our program, the coefficients for the case of perfect conductors ($\epsilon(\omega) \rightarrow -\infty$, which gives $\chi(\omega) = -1$) and compare the numerical results to the exact values, that can be obtained – for this limiting case – analytically. We request that n_{\max} be such that the two sets of coefficients coincide. (4) By taking $\epsilon(\omega) = \epsilon_0$ for one of the spheres, we make that sphere disappear. Then we request that the numerical results for that limiting case coincide – for the n_{\max} used – to the known one sphere results. (5) Finally, we derive a sum rule by requiring that the total induced surface charge on either sphere be zero (the volume polarization charge is zero). The surface charge density is

$$\sigma_s = \mathbf{P} \cdot \hat{n}, \quad (10)$$

where \hat{n} is the unit vector normal to the surface, and

$$\mathbf{P} = \frac{\epsilon(\omega) - 1}{4\pi} \mathbf{E} = - \frac{\epsilon(\omega) - 1}{4\pi} \nabla\Phi. \quad (11)$$

We get

$$\sigma_s = \frac{\epsilon_2(\omega) - 1}{4\pi} \frac{1}{h_\mu} \left. \frac{\partial\Phi_2}{\partial\mu} \right|_{\mu=\mu_0} \quad (12)$$

(here $\epsilon_2(\omega)$ is the dielectric constant of the metal in sphere 2). Requiring that the total induced charge on sphere 2 be zero leads to the condition

$$\sum_{n=0}^{\infty} A_n^0 (2n+1)^{1/2} = 0. \quad (13)$$

Similarly, the neutrality of sphere 1 leads to the condition

$$\sum_{n=0}^{\infty} B_n^0 (2n+1)^{1/2} = 0. \quad (14)$$

No conditions can be obtained for $A_n^{\pm 1}$ and $B_n^{\pm 1}$ since symmetry requirements cancel exactly the terms, in the total charge expression, which contain these coefficients. To test convergence we require that n_{\max} be such that the eqs. (13) and (14) are satisfied with very high accuracy.

In fig. 2 we present numerical results for the quantity \tilde{I} defined by eq. (7), as a function of the frequency of the incident field, for various “scale factors” λ . The

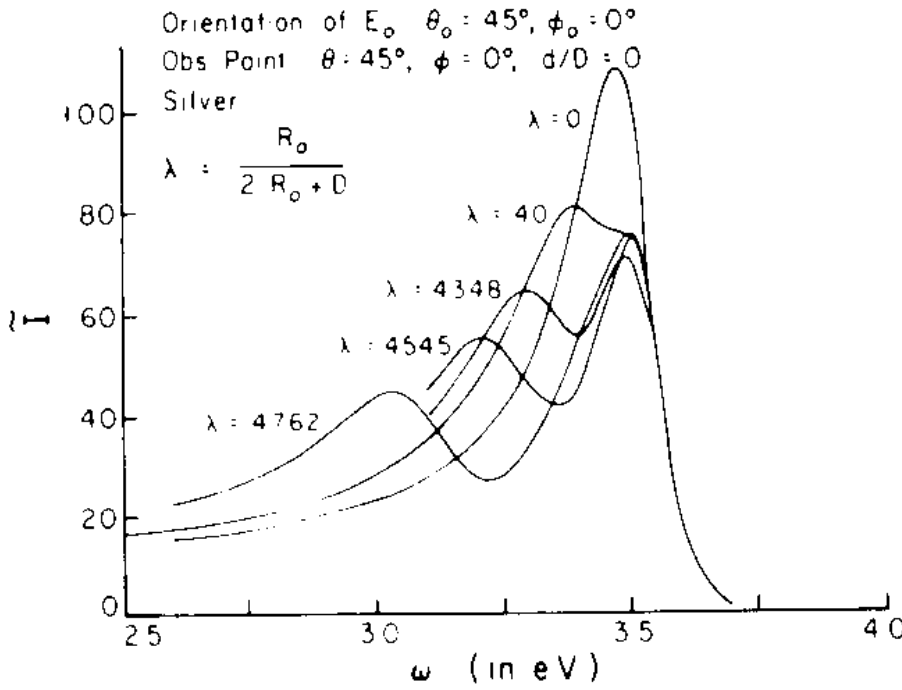


Fig. 2. Resonances of the 2-sphere system for different scale factors λ . For each λ , the intensity enhancement at the observation point, \tilde{I} , has been shown as a function of external frequency and two resonances can be clearly discerned.

external field in all these calculations is taken to have the direction specified by the azimuthal angle $\phi_0 = 0$ (in the xz plane) and the polar angle $\theta_0 = 45^\circ$ (see fig. 1). We assume that the dielectric constant of the spheres is that of the bulk silver [21]. We compute \tilde{I} at the point specified in fig. 1, for $d = 0$. The observation point is contained in the xz plane, (as is the incident field), on the surface of the sphere 2 at a polar angle $\theta = 45^\circ$.

The position of resonance frequency does not depend – for reasons explained in the previous section – on the point of observation or the angle of incidence. Curve 1 ($\lambda = 0$) shows \tilde{I} when the spheres are at infinite separation. Hence the curve represents \tilde{I} for the case of an isolated sphere. The resonance frequency satisfies the condition $\epsilon(\omega) + 2 = 0$, which for silver yields $\omega_{res} = 3.48$ eV.

As the spheres are brought closer (λ is increased) the resonance starts splitting into two peaks. The high frequency peak remains practically at $\omega \sim 3.48$ eV while the low frequency peak shifts downwards with λ . Furthermore the peak intensity for the low frequency resonance decreases with λ .

Qualitatively one can understand this splitting from the discussion presented in the Introduction. The two degenerate resonances of the isolated spheres couple to each other and the degeneracy is removed, resulting in splitting. One can also think that the two sphere system is – very crudely – similar to a prolate spheroid, which is known to have two resonances [22].

The curves in fig. 2 seem to imply that the coupling between spheres lowers the value of \tilde{I} on resonance (for the high frequency peak) as compared to the single sphere case, while raising it above the single sphere value, when the outside frequency corresponds to the lower frequency resonance. This situation is however

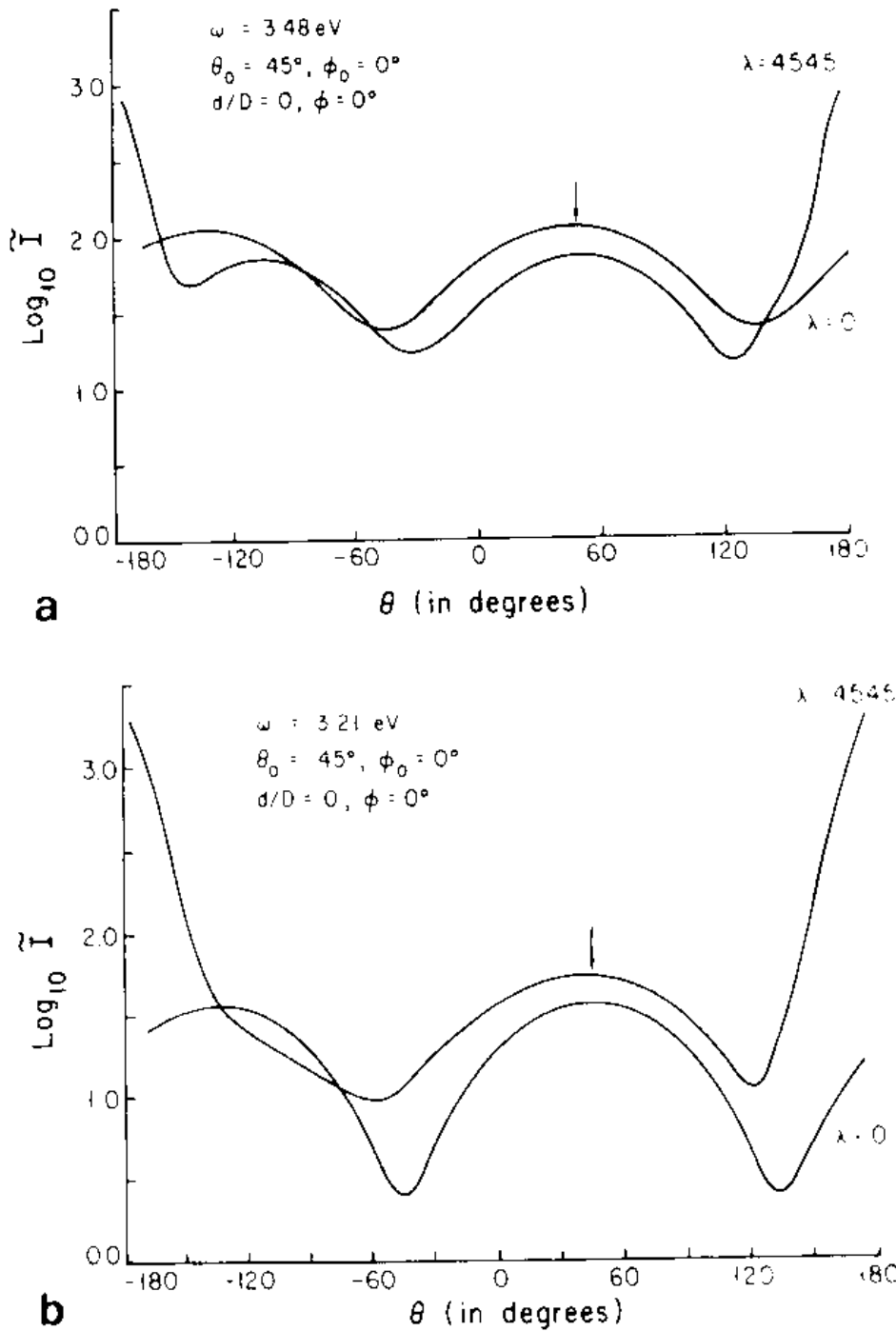
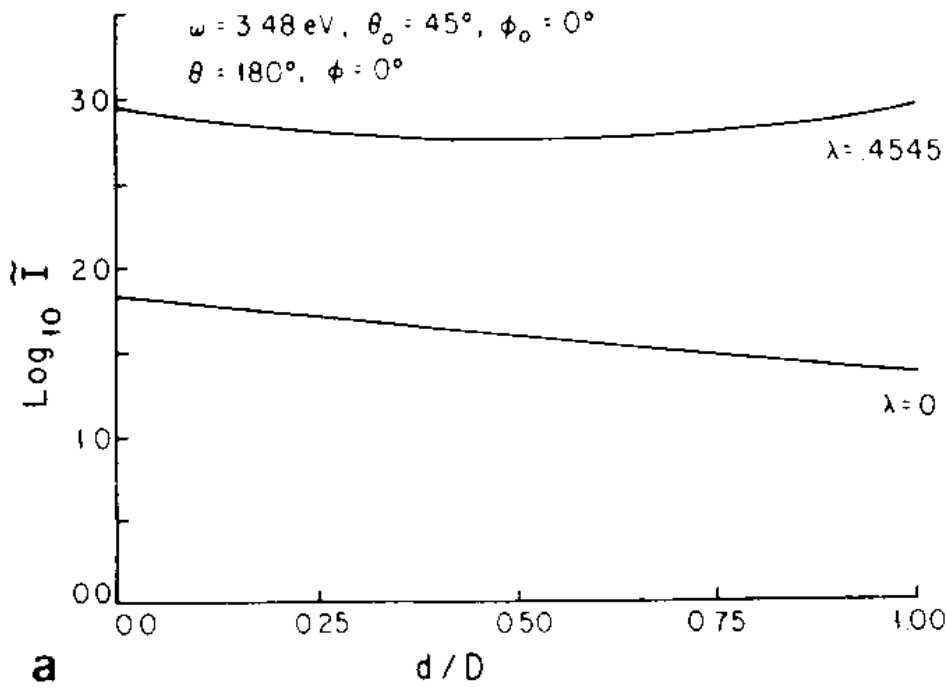


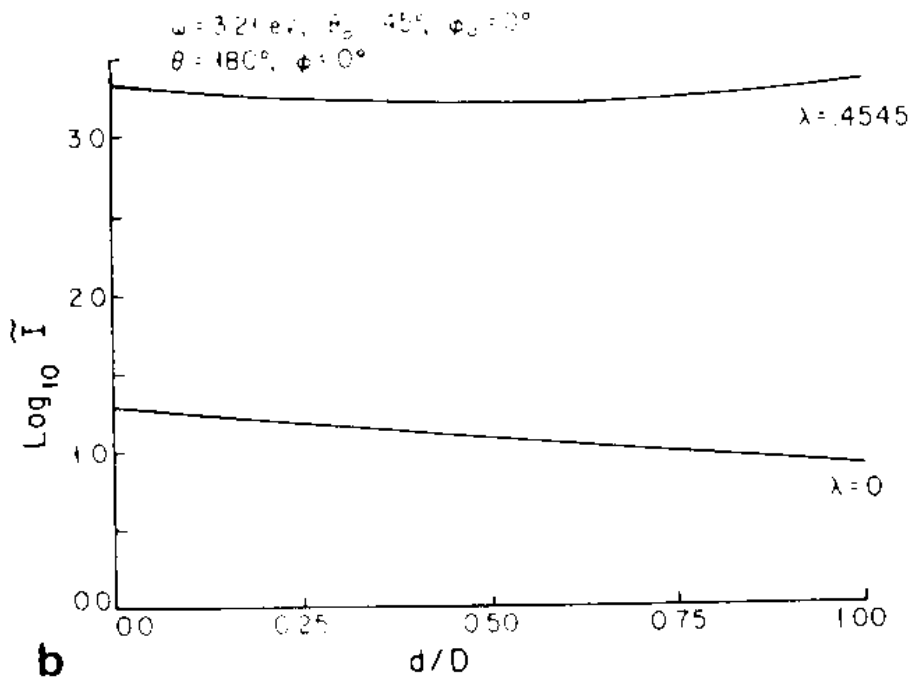
Fig. 3. (a) Plot of \tilde{I} (on a log scale) versus polar angle of observation point, θ , for the 2-sphere system $\lambda = 0.4545$ and the isolated sphere $\lambda = 0$. The external frequency $\omega = 3.48 \text{ eV}$ is at resonance for the isolated sphere and also very close to the upper resonance of the 2-sphere system. Arrow in figure is along the direction of the external field, in this case 45° . (b) Same as (a) but for $\omega = 3.21 \text{ eV}$, the lower resonance frequency of the 2-sphere system with $\lambda = 0.4545$.

peculiar to the observation point chosen in this graph, which happens to be in a position where the resonance value of \tilde{I} is maximum for a single sphere. In what follows we inquire into the dependence of \tilde{I} on the observation point.

In figs. 3a and 3b we look at the change of $\log_{10}\tilde{I}$ as a function of the polar angle. We keep the observation point in the plane xz at $d = 0$ and change θ to move it around the sphere 2. In fig. 3a we compare the curve $\log_{10}\tilde{I}$ versus θ for $\omega = 3.48 \text{ eV}$ (which corresponds to the high frequency resonance and also to the resonance



a



b

Fig. 4. (a) The upper curve, which is for the 2-sphere system $\lambda = 0.4545$, is a plot of \tilde{I} (on a log scale) versus distance d/D as one proceeds from the surface of one sphere to the other along their common axis. The lower curve is for the isolated sphere $\lambda = 0$ and the abscissa for this case should be read Sd/R_0 rather than d/D as shown. The external frequency $\omega = 3.48 \text{ eV}$ is the resonance of the isolated sphere. (b) Same as (a) but for $\omega = 3.21 \text{ eV}$, the lower resonance frequency of the 2-sphere system with $\lambda = 0.4545$.

of the single sphere) for the single sphere curve ($\lambda = 0$) to that for two interacting spheres ($\lambda = 0.45$). For almost every angle the free sphere field is larger, except for angles close to 180° (in the region between spheres) where the interacting sphere system give a value of \tilde{I} of roughly an order of magnitude larger than that for a single sphere.

In fig. 3b we make the same plot for the frequency $\omega = 3.21 \text{ eV}$, which corre-

sponds to the low frequency resonance for $\lambda = 0.45$. The isolated sphere does not have a resonance at this frequency. For this case the values of \tilde{I} for the interacting spheres is larger than that for a single sphere. At angles close to 180° (in the region between the spheres) \tilde{I} becomes very large.

In conclusion, the field in the region between spheres is substantially enhanced by the interaction between them. At a frequency corresponding to the single sphere resonance, the interaction between the spheres tends to depress the field in all regions except those located between them. At frequencies corresponding to the low energy resonance (absent in the single sphere case) the field is enhanced above the single sphere values, for practically all angles.

In figs. 4a and 4b we plot $\log_{10}\tilde{I}$ as a function of the distance d between the observation point and the surface of the sphere 2 (see fig. 1), along the line joining the centers ($\theta = 180^\circ$). For both frequencies ($\omega = 3.48$ eV and $\omega = 3.21$ eV) the intensity \tilde{I} for the interacting spheres ($\lambda = 0.45$) is substantially higher than that of the single sphere case. The enhancement is larger for frequencies corresponding to the low frequency resonance.

Of course the results will also vary with the angle of incidence, and intuitively one expects a very large enhancement in the region between spheres if $\theta_0 = 0$. It probably goes down if $\theta_0 = 90^\circ$.

4. Summary

The present calculations show the following. (1) The electromagnetic interaction between two silver spheres is long ranged. It has noticeable optical effects on the local field at a value of $\lambda = 0.4$, which corresponds to surface distance $D = R_0/2$. (2) The dependence of optical properties of the pair on the separation between the spheres is strong. A new resonance appears, at smaller frequencies than in the single sphere case; the splitting grows as the interparticle distance is diminished. In principle, this can be used to study the interparticle separation in colloidal solutions of low concentration (so that, in any "snap-shot" of the system most spheres are either isolated ($0 < \lambda \lesssim 0.3$) or form pairs ($\lambda \gtrsim 0.3$) and the number of "triplets" is very low. (3) The local field in the space between the two spheres is substantially enhanced by their electromagnetic interaction. This field is very large at frequencies corresponding to the low energy resonance of the two sphere system even though such frequencies are well below the single sphere resonance. (4) The local intensity in regions outside the space between spheres is lowered (as compared to the single sphere case) by the electromagnetic interaction, if the frequency is close to the single sphere resonance. It is increased (as compared to the single sphere case) if the frequency is at the low energy resonance.

We emphasize that Ag is a rather special material [23] for which the electromagnetic resonances have very small damping. Au, Cu, Hg are similar, but have larger damping. As a result their ability to generate large resonant local fields is smaller.

Acknowledgement

We are grateful to National Science Foundation for the support of this work. We had useful discussions with Arnie Adams, Paul Hansma, Milton Kerker and Doug Scalapino. One of us (A.N.) had extensive and useful discussions with Joel Gersten concerning this problem.

Appendix

We give here the linear equations determining the expansion coefficients A_n^m , B_n^m , C_n^m and D_n^m occurring in eqs. (1) of the text. The desired equations are obtained directly from the electrostatic boundary conditions (3) and (4). Before quoting the results we mention a number of simplifying features that expedite the solution of the problem: (a) as explained in the text, the constancy of the external electric field, eq. (2), leads to only the $m = 0$ and $m = \pm 1$ modes appearing in the solution; (b) the symmetry of the system with respect to its midplane ($\mu = 0$) leads to the following relations among the expansion coefficients:

$$A_n^0 = -B_n^0, \quad C_n^0 = -D_n^0, \tag{A.1}$$

$$A_n^{\pm 1} = B_n^{\pm 1}, \quad C_n^{\pm 1} = D_n^{\pm 1}; \tag{A.2}$$

(c) the symmetry of the system about the common axis of the two spheres leads to the following connection between the $m = +1$ and $m = -1$ modes:

$$\begin{pmatrix} A_n^{-1} \\ C_n^{-1} \end{pmatrix} = -\exp(2i\phi_0) \begin{pmatrix} A_n^1 \\ C_n^1 \end{pmatrix}. \tag{A.3}$$

As a consequence of (b) we need consider only the boundary conditions (3a) and (4a) and, further, as a result of (a) and (c), we need only apply them to the $m = 0$ and $m = +1$ modes. On doing this we obtain the following sets of equations for the expansion coefficients in the different modes.

m = 0 mode

$$U_n^0 A_n^0 + V_n^0 A_{n-1}^0 + W_n^0 A_{n+1}^0 = S_n^0, \tag{A.4a}$$

where

$$U_n^0 = \chi \sinh \mu_0 \{1 - \exp[-(2n+1)\mu_0]\} + (2n+1) \cosh \mu_0 \{1 + \chi \exp[-(2n+1)\mu_0]\}, \tag{A.4b}$$

$$V_n^0 = -n \left(\frac{2n-1}{2n+1} \right)^{1/2} \exp(-\mu_0) \{1 + \chi \exp[-(2n-1)\mu_0]\}, \tag{A.4c}$$

$$W_n^0 = -(n+1) \left(\frac{2n+3}{2n+1} \right)^{1/2} \exp(\mu_0) \{1 + \chi \exp[-(2n+3)\mu_0]\}, \quad (\text{A.4d})$$

$$S_n^0 = 2F_0 \cos \theta_0 \chi \exp[-(2n+1)\mu_0] \left(\frac{4\pi}{2n+1} \right)^{1/2} \{\cosh \bar{\mu}_0 - (2n+1) \sinh \mu_0\}. \quad (\text{A.4e})$$

The notation $F_0 \equiv c_0 E_0 \sqrt{2}$ and $\chi \equiv [\epsilon_0 - \epsilon(\omega)] [\epsilon_0 + \epsilon(\omega)]^{-1}$ has been used. C_n^0 is given in terms of A_n^0 by

$$C_n^0 = \{\exp[(2n+1)\mu_0] - 1\} A_n^0 - F_0 \cos \theta_0 [4\pi(2n+1)]^{1/2}. \quad (\text{A.4f})$$

$m = +1$ mode

$$U_n^1 A_n^1 + V_n^1 A_{n-1}^1 + W_n^1 A_{n+1}^1 = S_n^1, \quad (\text{A.5a})$$

where

$$U_n^1 = \chi \sinh \mu_0 \{1 + \exp[-(2n+1)\mu_0]\} + (2n+1) \cosh \mu_0 \{1 - \chi \exp[-(2n+1)\mu_0]\}, \quad (\text{A.5b})$$

$$V_n^1 = - \left(\frac{(n+1)(n-1)(2n-1)}{2n+1} \right)^{1/2} \exp(-\mu_0) \{1 - \chi \exp[-(2n-1)\mu_0]\}, \quad (\text{A.5c})$$

$$W_n^1 = - \left(\frac{n(n+2)(2n+3)}{2n+1} \right)^{1/2} \exp(\mu_0) \{1 - \chi \exp[-(2n+3)\mu_0]\}, \quad (\text{A.5d})$$

$$S_n^1 = 2F_0 \sin \theta_0 \sinh \mu_0 \chi \exp(-i\phi_0) \exp[-(2n+1)\mu_0] \left(\frac{4\pi n(n+1)}{2n+1} \right)^{1/2}. \quad (\text{A.5e})$$

C_n^1 is given in terms of A_n^1 by

$$C_n^1 = \{\exp[(2n+1)\mu_0] + 1\} A_n^1 + F_0 \sin \theta_0 \exp(-i\phi_0) \left(\frac{4\pi n(n+1)}{2n+1} \right)^{1/2}. \quad (\text{A.5f})$$

Eqs. (A.4) and (A.5) are linear difference equations of 2nd order for the expansion coefficients A_n^0 and A_n^1 . By choosing a suitably large cutoff in n (as discussed in the text), the equations can be reduced to finite matrix equations which are readily solved on a computer. Once the A 's are known the other coefficients, B , C and D may be found from (A.1), (A.2), (A.3), (A.4f) and (A.5f). This completes the solution of the boundary value problem.

References

[1] For use of gratings see:

- (a) J.C. Tsang, J.R. Kirtley and J.A. Bradley, Phys. Rev. Letters 43 (1979) 772; P.N. Sanda, J.W. Warlaumont, J.E. Demuth, J.C. Tsang, K. Christman and J.A. Bradley, Phys. Rev. Letters 45 (1980) 1519;

- (b) A. Girlando, M.R. Philpott, D. Heitmann, J.D. Swallen and R. Santo, *J. Chem. Phys.* 72 (1980) 5187;
- (c) J.R. Kirtley, J.C. Tsang, T.N. Theis and S.S. Jha, in: *Proc. 7th Intern. Raman Conf.*, Ed. W.F. Murphy (North-Holland, New York, 1980) p. 386; S.S. Jha, J.R. Kirtley and J.C. Tsang, *ibid.*, p. 356; A. Girlando, Z.G. Gordon II, D. Heitmann, M.R. Philpott, H. Seki and J.D. Swallen, *Surface Sci.* 101 (1980) 417.
- [2] For use of coarse roughness see:
J.E. Rowe, C.V. Shank, D.A. Swemer and C.A. Murray, *Phys. Rev. Letters* 44 (1980) 1770;
D.A. Swemer, C.V. Shank and J.E. Rowe, *Chem. Phys. Letters* 73 (1980) 201;
D.A. Weitz, T.J. Gramla, A.Z. Genack and J.I. Gersten, *Phys. Rev. Letters* 45 (1980) 355.
- [3] For the use of metal islands see:
C.Y. Chen, E. Burstein and S. Lundquist, *Solid State Commun.* 32 (1979) 63;
E. Burstein and C.Y. Chen, in: *Proc. 7th Intern. Raman Conf.*, Ed. W.F. Murphy (North-Holland, New York, 1980) p. 346;
C.Y. Chen, I. Davoli, G. Ritchie and E. Burstein, *Surface Sci.* 101 (1980) 363.
- [4] For tunneling junctions emission see:
P.K. Hansma, H.P. Broida, *Appl. Phys. Letters* 32 (1978) 545;
A. Adams, J.C. Wyss and P.K. Hansma, *Phys. Rev. Letters* 42 (1979) 912;
D. Hone, B. Mühlischlegel and D.J. Scalapino, *Appl. Phys. Letters* 33 (1978) 203;
R.W. Rendell, D.J. Scalapino and B. Mühlischlegel, *Phys. Rev. Letters* 41 (1978) 1746.
- [5] For recent use of attenuated total reflection to excite the surface plasmon and use it to enhance spectroscopic signals see:
A. Otto, *Surface Sci.* 101 (1980) 99;
B. Pettinger, A. Tadjeddine and D.H. Kolb, *Chem. Phys. Letters* 66 (1979) 544;
A. Tadjeddine, D.M. Kolb and R. Kotz, *Surface Sci.* 101 (1980) 277;
Y.G. Gordon II and S. Ernst, *Surface Sci.* 101 (1980) 499;
R. Dornhaus, R.F. Benner, R.K. Chang and I. Chabay, *Surface Sci.* 101 (1980) 367.
- [6] For use of colloidal solutions see:
(a) A. Creighton, C.B. Blatchford and M.G. Albrecht, *J. Chem. Soc. Faraday Trans. II*, 75 (1979) 790;
(b) M. Kerker, O. Siiman, L.A. Bumm and D.S. Wang, *Appl. Opt.* 19 (1980) 3253.
- [7] For the theory of spectroscopy on gratings see:
S.S. Jha, J.R. Kirtley and J.C. Tsang, *Phys. Rev. B* 22 (1980) 3973;
P.K. Aravind, E. Hood and H. Metiu, *Surface Sci.* 109 (1981) 95, and papers quoted therein.
- [8] For use of resonances of spheres see:
(a) J.I. Gersten, *J. Chem. Phys.* 72 (1980) 5779, 5780; S.L. McCall, P.M. Platzmann and P.A. Wolf, *Phys. Letters* 77A (1980) 381; S.L. McCall and P.M. Platzmann, *Phys. Rev. B* 22 (1980) 1660.
(b) D.S. Wang, H. Chew and M. Kerker, *Appl. Opt.* 19 (1980) 2256; M. Kerker, D.S. Wang and H. Chew, *Appl. Opt.* 19 (1980) 3373.
- [9] For ellipsoids on surfaces see:
A. Nitzan and J.I. Gersten, *J. Chem. Phys.* 73 (1980) 3023.
Spheres on surfaces were treated by P.K. Aravind, R. Rendell and H. Metiu, unpublished.
- [10] For metal islands see:
M. Moskovits, *J. Chem. Phys.* 69 (1978) 4159; *Solid State Commun.* 32 (1978) 59;
C.Y. Chen and E. Burstein, *Phys. Rev. Letters* 45 (1980) 1278.
- [11] For the theory of light emission by localized resonances in tunneling junctions see:
B. Laks and D.L. Mills, *Phys. Rev. B* 20 (1979) 4962; B21 (1980) 5175;
D. Hone, B. Mühlischlegel and D.J. Scalapino, *Appl. Phys. Letters* 33 (1978) 203;
R.W. Rendell, D.J. Scalapino and B. Mühlischlegel, *Phys. Rev. Letters* 41 (1978) 1746.

- [12] For emission spectroscopy near a randomly rough surface see:
P.K. Aravind and H. Metiu, *Chem. Phys. Letters* 74 (1980) 301.
- [13] C. Jedrzejek, K.F. Freed, S. Efrima and H. Metiu, *Surface Sci.* 109 (1981) 191.
- [14] L. Brus and A. Nitzan, *J. Chem. Phys.*, to be published.
- [15] R.R. Chance, A. Prock and R. Silbey, *Advan. Chem. Phys.* 37 (1978) 1.
- [16] S. Efrima and H. Metiu, *Surface Sci.* 92 (1980) 417; *J. Chem. Phys.* 70 (1979) 1939.
- [17] We quote a few papers that have addressed this problem.
Experimental:
J.D. Ganjere, R. Rechsteiner, M.A. Smithard, *Solid State Commun.* 16 (1975) 113;
L. Genzel, T.P. Martin, U. Kreibig, *Z. Physik B* 21 (1975) 339;
C.J. Duthler, S.E. Johnson and H.P. Broida, *Phys. Rev. Letters* 26 (1971) 1236;
S. Norman, T. Anderson, C.G. Ganqvist and O. Hunderi, *Phys. Rev. B* 18 (1978) 674;
P. Ascarelli and M. Cini, *Solid State Commun.* 18 (1976) 385.
Theoretical: M. Cini and P. Ascarelli, *J. Phys. F. (Metal Phys.)* 4 (1974) 1998;
R. Ruppin and H. Yatom, *Phys. Status Solidi (b)* 74 (1976) 674.
- [18] A. Schmidt-Ott, P. Schurtenberger and H.C. Siegmann, *Phys. Rev. Letters* 45 (1980) 1248.
- [19] P.M. Morse and H. Feshbach, *Methods of Theoretical Physics* (McGraw-Hill, New York, 1953) p. 1298.
The problem has been previously discussed in the literature in a rather formal way: V. Twersky, *J. Math. Phys.* 8 (1967) 589; S. Levine and G.O. Olaofe, *J. Colloid Interface Sci.* 27 (1968) 442.
For our present purpose it seems simpler to generate a numerical procedure by solving the problem anew with the method outlined by Morse and Feshbach.
- [20] J.D. Jackson, *Classical Electrodynamics* (Wiley, New York, 1975) p. 98.
- [21] H.J. Hagemann, W. Gudat and C. Kunz, *DESY Report*, No. SR-74/7 (May 1974).
- [22] See for example, D.C. Skillman and C.R. Berry, *J. Chem. Phys.* 48 (1968) 3297.
- [23] H. Ehrenreich and H.R. Philipp, *Phys. Rev.* 128 (1962) 1622.